PERGAMON

Journal of Structural Geology 23 (2001) 1441–1456

JOURNAL OF STRUCTURAL GEOLOGY

www.elsevier.com/locate/jstrugeo

Incremental strain analysis using two generations of syntectonic coaxial fibres: an example from the Monte Marguareis Briançonnais Cover nappe (Ligurian Alps, Italy)

Eugenio Carminati*

Dipartimento di Scienze della Terra, Università degli Studi di Milano, Via Cicognara 7, I-20129 Milan, Italy

Received 3 April 2000; revised 28 December 2000; accepted 11 January 2001

Abstract

Composite calcite–quartz fibres, developed in strain fringes on pyrites in the Monte Marguareis cover nappe (Ligurian Briançonnais, Northern Italy), are utilised for an incremental strain analysis. Classical methods require non-coaxial fibres to reconstruct incremental strain histories. As an innovation this contribution shows that two generations of coaxial fibres grew independently on different pyrite sites during the two major deformation phases (D1 and D2) which affected the Monte Marguareis structural unit. Rare curved fibres are shown by meso- and microstructural analyses to have grown during D1 and been deformed by D2 folds. This peculiarity provides a way to estimate, quantitatively, the strain associated with these deformation phases without the uncertainties related to classical methods. D1 strain shows a marked strain partitioning among different lithologies and within the same lithology, the measured elongations ranging between 1.84 and 8.45. Measurements of D2 incremental elongation are available only for one lithology and indicate that D2 stretching is approximately half that of D1 and its contribution to the finite strain ellipsoid cannot be neglected. This finding is consistent with qualitative inferences on strain partitioning between D1 and D2 phases. Measured D2 elongations display higher homogeneity throughout the area.

Both L1 fibre orientation (generally NE–SW) and D1 fold asymmetry suggest D1 deformation occurred in a ductile shear zone possibly induced by the south-westward motion of nappes, consistently with regional tectonics. The L2 lineation orientation (approximately NE–SW) and the D2 folds asymmetry suggest that the D2 phase is likely to be the product of a regionally recognised backthrusting event.

1. Introduction

The measurement of finite strain within strongly deformed thrust sheets of the Briançonnais domain (Western Alps, Italy) has been performed by several authors (e.g. Menardi-Noguera, 1988; Seno, 1992). Recently Seno et al. (1998) tried to fill in the gap between bulk strain and incremental strain measurements by subdividing the measured bulk strain into increments by means of computer simulations. The present contribution aims at filling the same gap, for the Monte Marguareis Briançonnais unit, with the analysis of syntectonic fibres.

Many methods using syntectonic fibres for determining incremental strain histories have been proposed (e.g. Spencer, 1991 and references therein). All of these methods make use of curved fibres which are assumed to be syntectonic and not affected by subsequent deformation. Consequently, the fibres are considered to remain rigid or behave passively during deformation subsequent to their formation (e.g. Durney and Ramsay, 1973; Ramsay and Huber, 1983, p. 270). Although these methods have been successfully applied in several areas (e.g. Dietrich, 1989 for the Alps), the validity of this assumption has been in some cases disputed. White and Wilson (1978), for example, showed that, within pressure fringes on magnetites from Mount Isa, curved quartz fibres displayed an increase in dislocation densities away from the magnetite grain and suggested that fibre curvature had been induced by deformation following the fibre formation. Caution is therefore required when utilising curved fibres to determine strain histories.

In this paper, it will be shown that the composite calcite–quartz fibres developed in strain fringes on pyrites in the Monte Marguareis cover nappe permit a strain history reconstruction without the uncertainties summarised above. It will be, in fact, proved that two generations of coaxial fibres grew independently during the two major deformation phases which affected the Monte Marguareis

* Now at: Dipartimento di Scienze della Terra, Università degli Studi di Roma "La Sapienza", P. le Aldo Moro 5, I-00185 Rome, Italy. Tel.: +39-06-49914950, fax: +39-06-4454729.

E-mail address: eugenio.carminati@uniroma1.it (E. Carminati).

0191-8141/01/$ - see front matter
PII: S0191-8141(01)00010-4

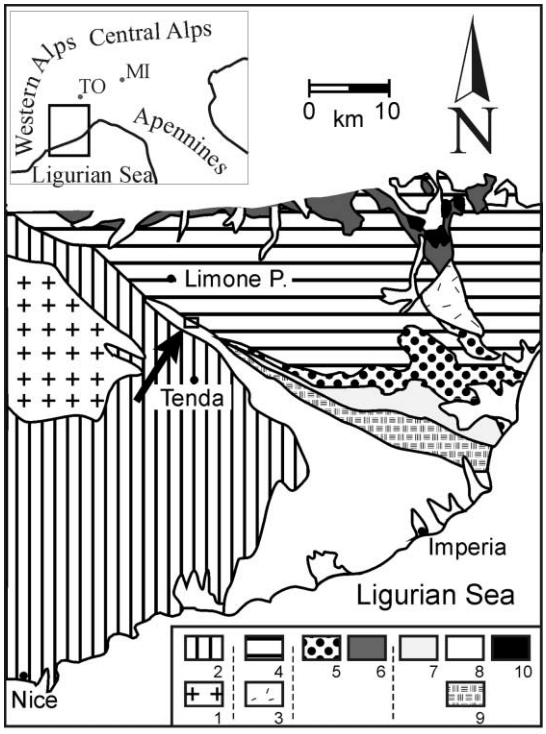

Fig. 1. Simplified map of the Ligurian Maritime Alps. The rectangle indicated by the black arrow delimits the study area. *European domain* (Basement and post-Hercynian cover). 1: Argentera–Mercantour massif; 2: Dauphinois, Subbriançonnais; 3: Calizzano–Savona unit; 4: Briançonnais units; 5–6: Prepiemontais and external Piemontais of the Arnasco–Castelbianco and Case Tuberto units (5) and of the M. Motta type and external Piemontais Schistes Lustrès units (6). *Oceanic domain* (Flysches). 7: Borghetto d'Arroscia–Alassio unit; 8: San Remo–Monte Saccarello unit; 9: Moglio–Testico unit; 10: Ophiolites. Modified after Brizio et al. (1983).

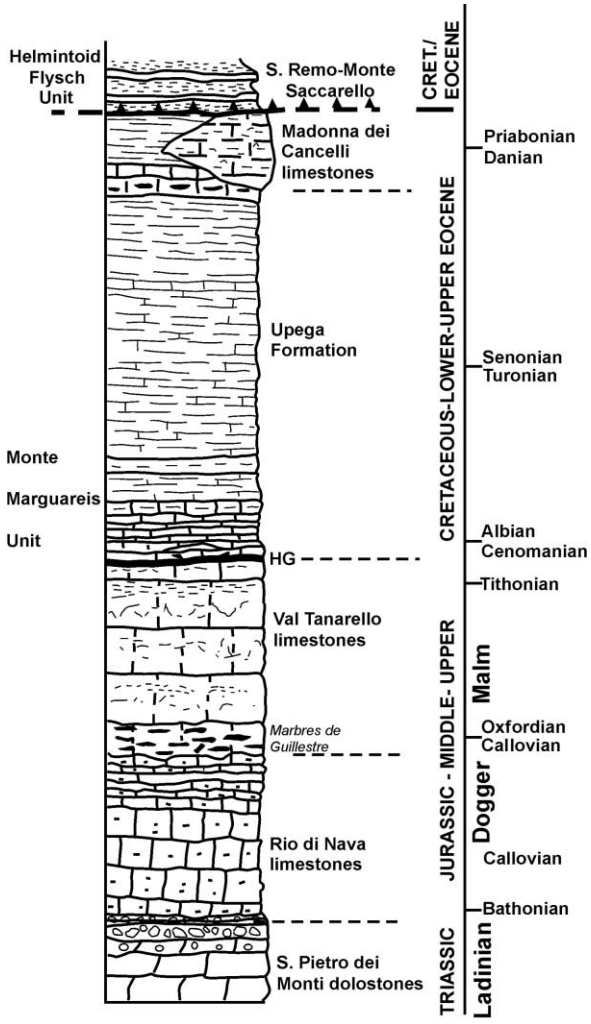

Fig. 2. Sketched stratigraphic sequence of the Ligurian–Briançonnais sediments of the Monte Marguareis Unit and of the basal complex of the San Remo–Saccarello unit of Helminthoid Flysch (modified after Brizio et al. (1983)). The San Pietro dei Monti Dolostones consist of dark dolomitic limestones, dolomitic–calcareous intraformational breccias and pale coloured dolostones, Triassic (Anisian–Ladinian) in age. Bathonian–Oxfordian Rio di Nava Limestones are dark, foliated to massive limestones. They are bounded to the top by a laterally continuous cm- to 10-m-thick cherty limestone of Callovian–Oxfordian age (Gosso et al., 1983). This layer is followed by the Val Tanarello Limestones (Oxfordian–Titonian) which are grey, pink or pale-brown limestones, locally nodular, corresponding to the Marbres de Guillestre of the classical Briançonnais zone. They are bounded to the top by a phosphatic-stromatolitic hard ground of Albian–Cenomanian age. Late Cretaceous–Paleocene sequences are marly, slightly arenaceous, limestones with pelitic and arenaceous beds and graphitic slates, equivalent to the *Calcschistes Planctoniques* of the classical Briançonnais Upega Formation. The uppermost unit of the MMU succession within the study area is the Madonna dei Cancelli Limestones, dark massive fossiliferous calcarenitic limestones of Paleocene–Late Eocene age. The San Remo–Monte Saccarello unit of the Helminthoid Flysch consists, in the Monte Marguareis area, of its Basal Complex, made up of red to green slates of Senonian (?) age.

structural unit. This peculiarity provides a way to estimate, quantitatively, the strains associated with the deformation phases, which appear to be consistent with qualitative observations collected during structural mapping of the area.

2. Structural setting

The Monte Marguareis area is located in the Ligurian Alps, which constitutes the southernmost segment of the Western Alps (Fig. 1). The Western Alps' structural (e.g. Vanossi et al., 1984) and metamorphic (e.g. Messiga et al., 1981) assemblage came about during convergence and collision between the Adria microplate and Europe from the late Cretaceous onwards (Dewey et al., 1989). During the Oligocene–Miocene this tectonometamorphic assemblage became involved in the Apenninic kinematic system and was thrusted to the north-east (Laubscher et al., 1992).

The Monte Marguareis massif is a glacio-karstic area where a complex sandwich of Briançonnais rocks belonging to the Monte Marguareis Unit and turbidite sequences of the

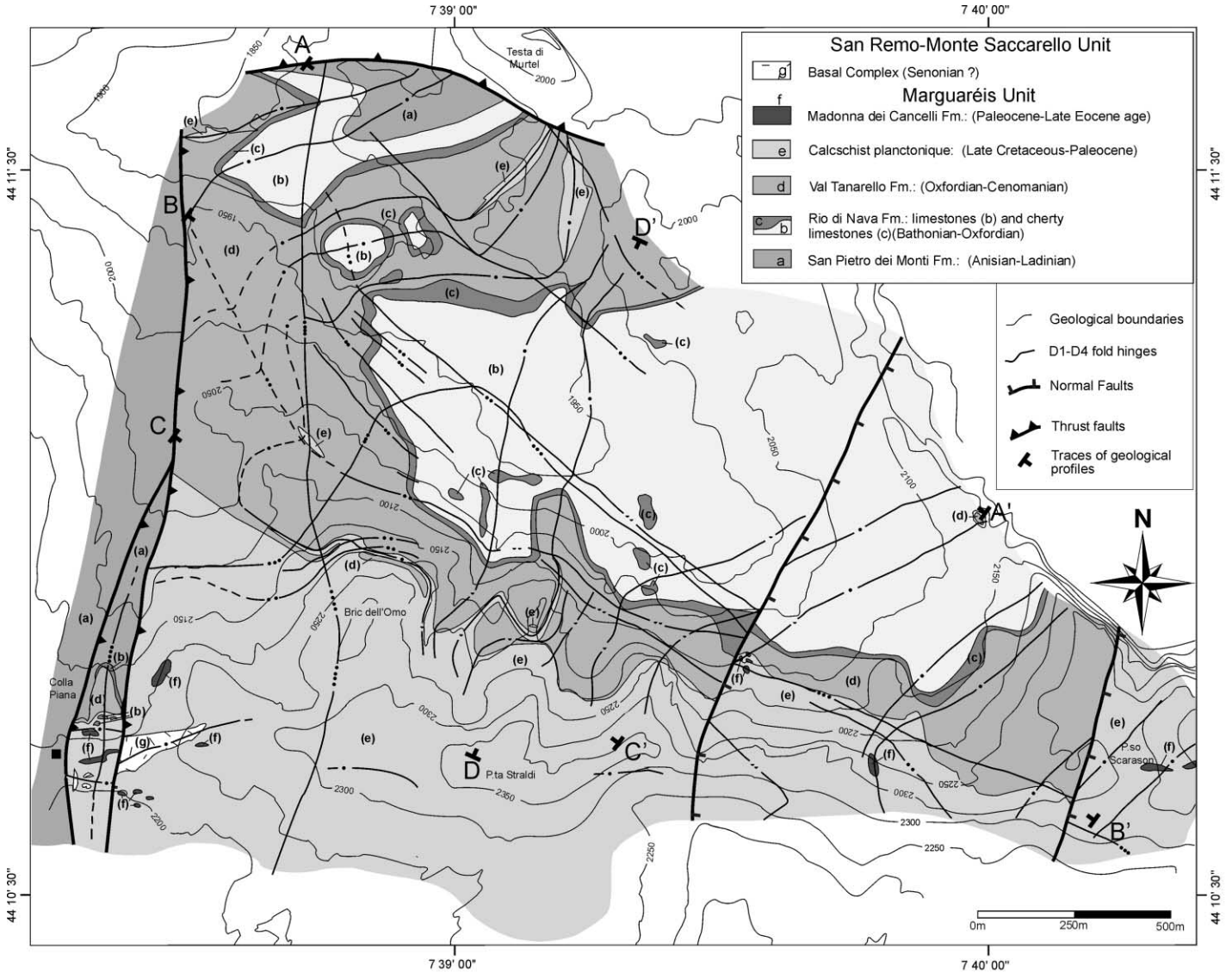

Fig. 3. Structural map of the Conca delle Carsene area, Monte Marguareis Massif. (a) Lithology distribution and major structures (fold axes and faults). (b) Measurements of D1 fabric elements, traces of D1 planar fabric elements and traces interpolations. Location and results of strain analyses performed on D1 stretching lineations are also shown. (c) Measurements of D2 fabric elements, traces of D2 planar fabric elements and their interpolated traces. Location and results of strain analyses performed on D2 stretching lineations are also shown. Interpolated traces in panels (b) and (c) are portrayed only for the areas where a well developed D1 or D2 cleavage has been observed.

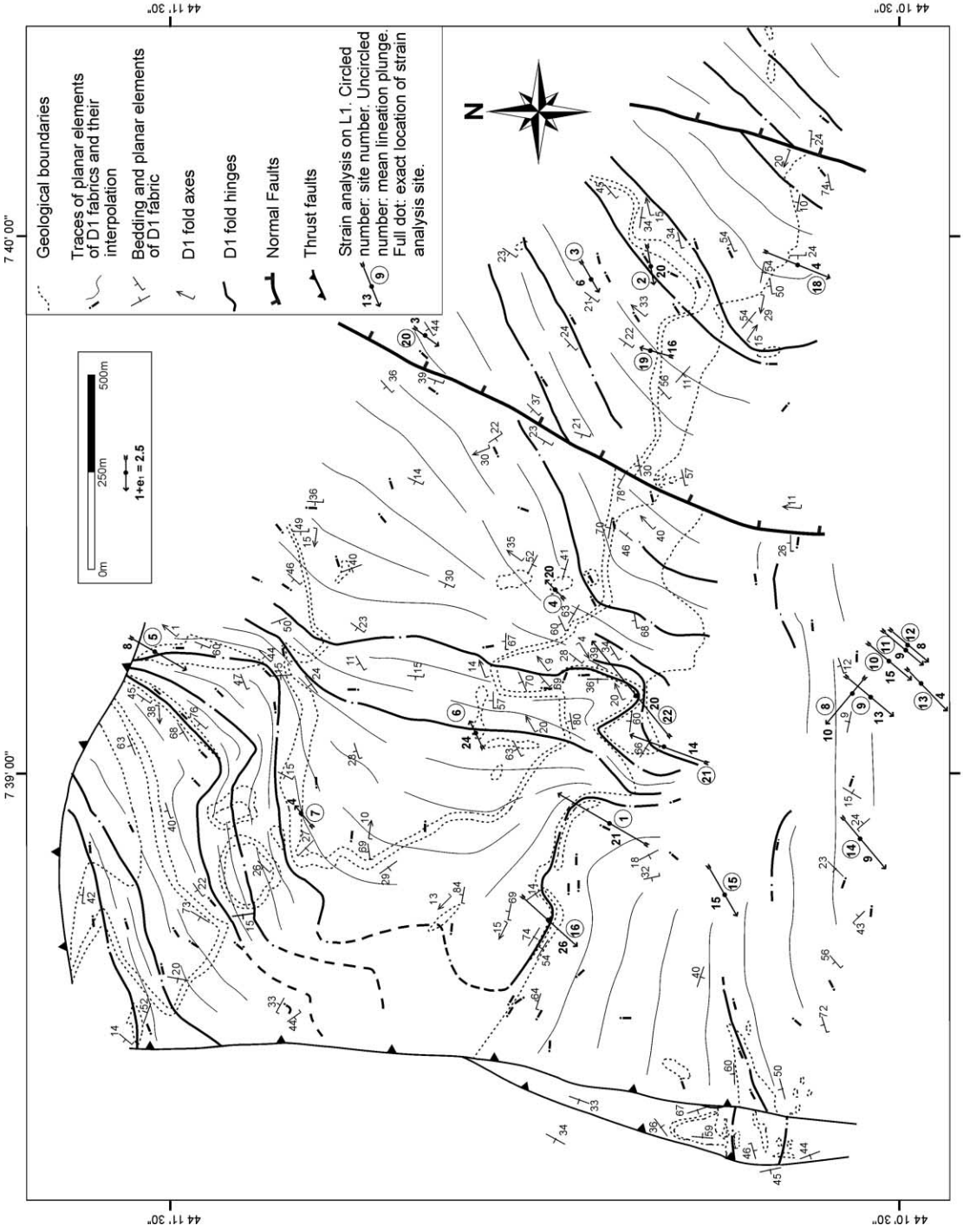

Fig. 3. (*continued*)

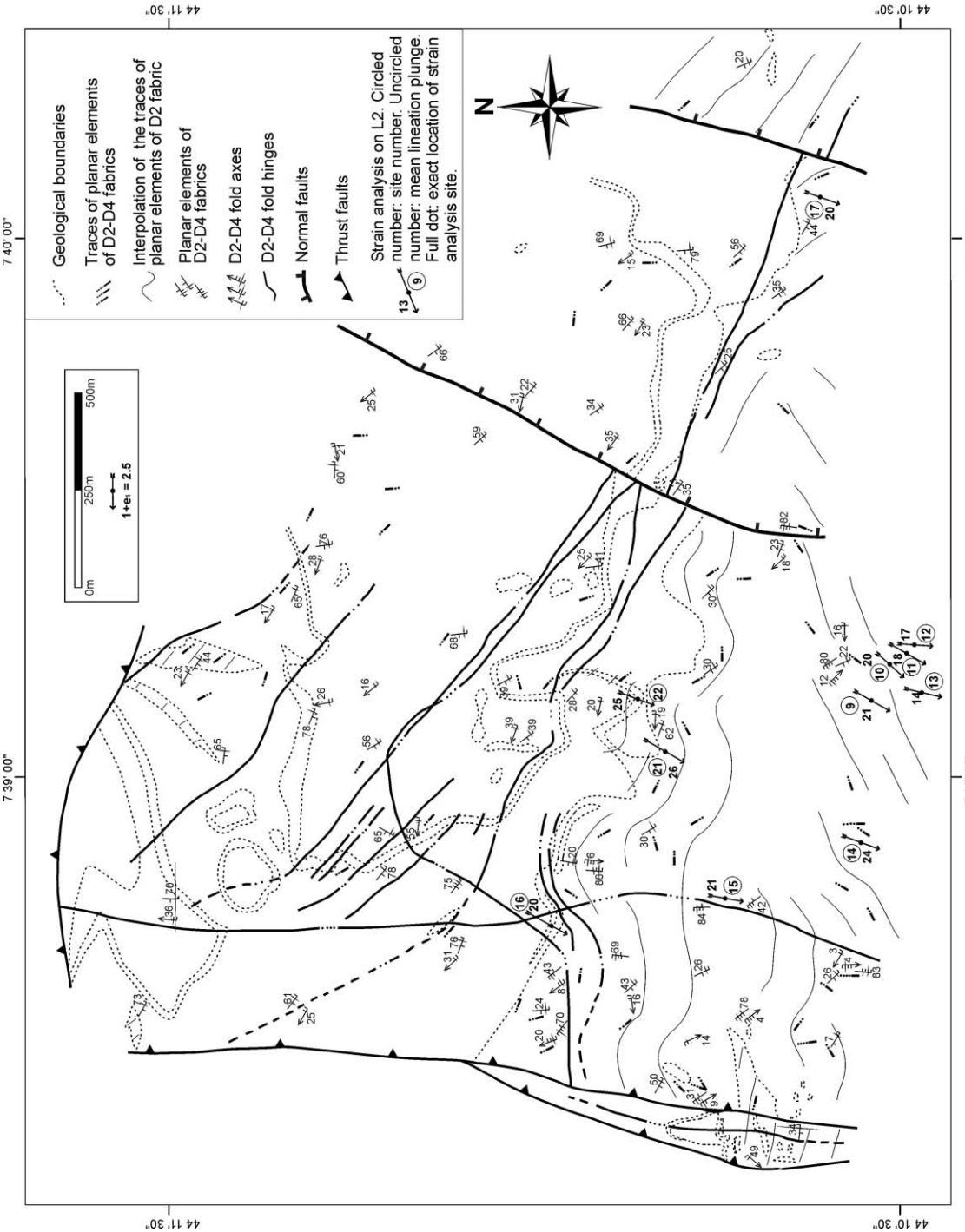

Fig. 3. (*continued*)

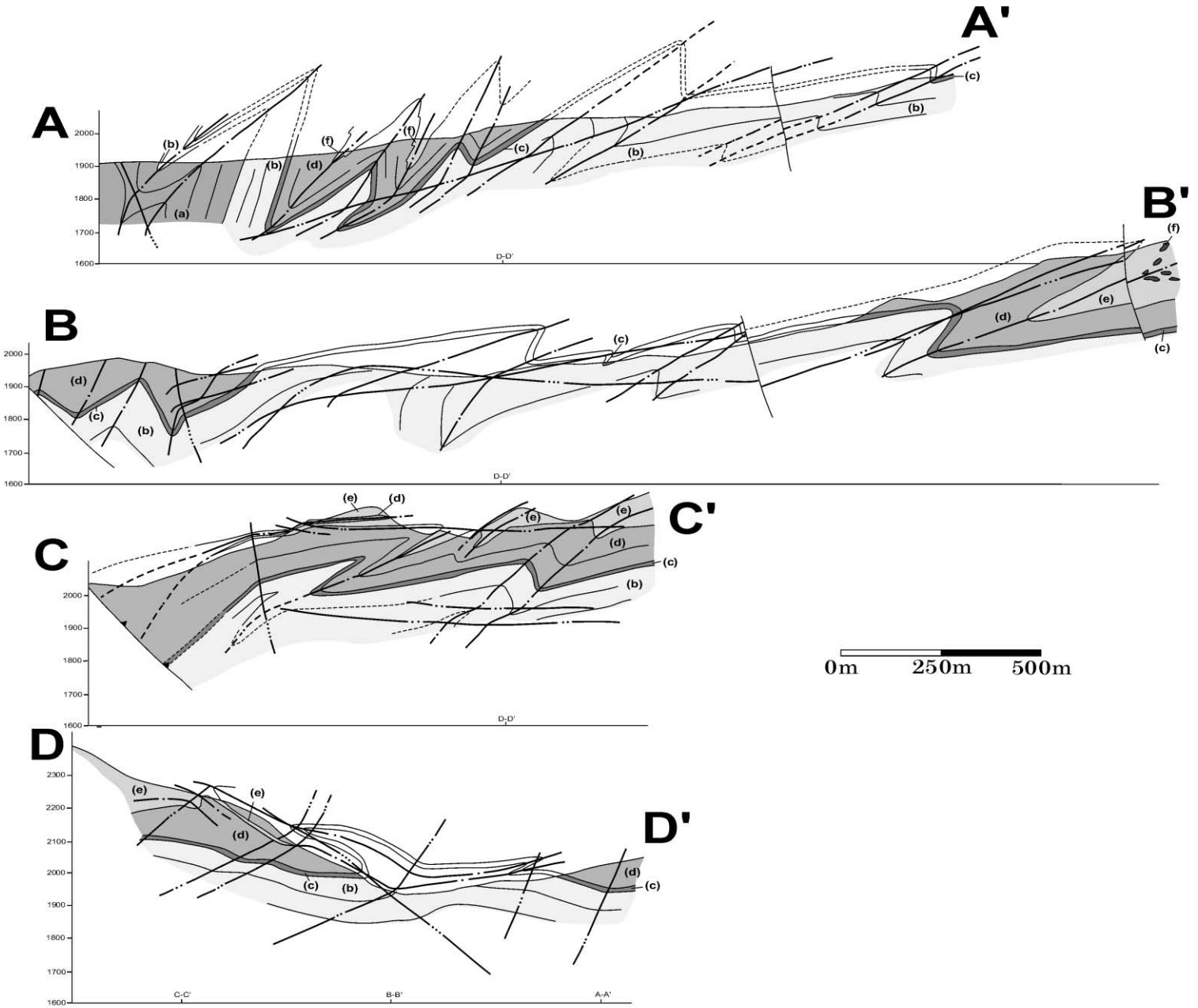

Fig. 4. Geological cross-sections through the Conca delle Carsene area, Monte Marguareis Massif. Their locations are indicated in Fig. 3. Lithologies are shaded and labelled as in Fig. 3a.

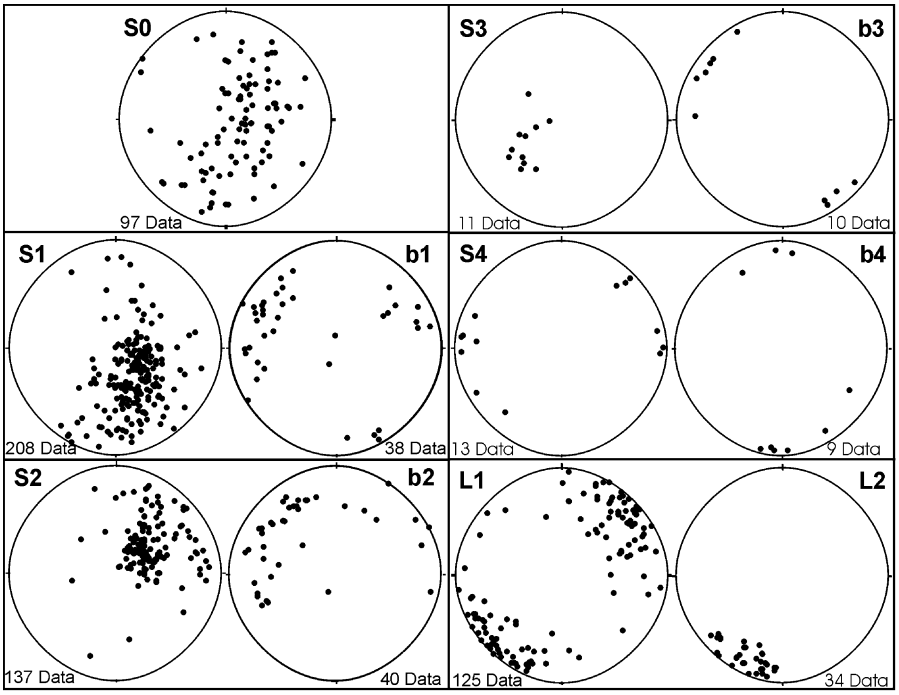

Fig. 5. Schmidt projection (lower hemisphere) of bedding, D1–D4 fabric elements and L1–L2 stretching lineations. S1 and S2 are fold axial planes and axial plane cleavages of D1 and D2 phases, respectively. S3 and S4 are fold axial planes of D3 and D4 phases, respectively. B1 and B4 are axes of D1 and D4 folds, respectively.

San Remo–Monte Saccarello unit of the Helminthoid Flysch (Manivit and Prud'Homme, 1990) occurs. The Monte Marguareis Unit (MMU) is a middle Triassic to Eocene Briançonnais cover nappe (Guillaume, 1969; Vanossi, 1972). The stratigraphic sequence of the MMU in the Monte Marguareis area is shown in Fig. 2. The San Remo–Monte Saccarello unit of the Helminthoid Flysch consists, in the Monte Marguareis area, of its Basal Complex, made up of red to green slates of Senonian (?) age.

2.1. Deformation history

In the Monte Marguareis area, polyphase tectonic interlayering and interfolding led to the present complex 3D geometry unravelled by Brizio et al. (1983) and Carminati and Gosso (2000). The strain analysis discussed in this paper has been performed in the Conca delle Carsene area (Fig. 1) and relies on a detailed structural analysis (surface mapping at 1:5000 scale), which led to the recognition (from kilometre to centimetre scale) of four folding events (D1–D4) on the basis of overprinting criteria, folding style and fabric orientation. The structural assemblage of the Conca delle Carsene area is summarised in the maps of Fig. 3 and in the cross-sections of Fig. 4.

D1 deformation often produces duplications of the MMU succession between the Rio di Nava Limestones and Madonna dei Cancelli Limestones but also affects the Triassic San Pietro dei Monti Dolostones and the overlying Helminthoid Flysch nappe. D1 structures (Figs. 3b and 4) are overturned folds, sometimes isoclinal, with axial planes generally dipping 10–60° towards the north (Fig. 5) and constant *S*-asymmetry (looking from N to S). Rare D1 sheath folds were observed in the extremely ductile cherty limestone at the top of the Rio di Nava Limestones. An axial plane cleavage (S1) commonly developed during D1 folding. Its morphology (Powell, 1979) and pervasiveness are functions of the lithology. A mm-spaced to continuous pervasive cleavage is associated with D1 folds in Cretaceous marly limestones of the Upega Formation, whereas a mm- to cm-spaced cleavage develops in the Rio di Nava Limestones. Locally, a cm-spaced fracture cleavage developed in normally massive, white Val Tanarello Limestones. Extremely rare foliations are observed in Triassic San Pietro dei Monti Dolostones and in Madonna dei Cancelli Limestones. Fig. 3b displays D1 fabric elements with the traces (intersection between foliation and topography) of the D1 planar fabric elements.

D2 deformation usually consists of open to tight chevron folds with axial planes gently to steeply dipping to the south (Figs. 3c, 4 and 5). D2 folds have a constant (looking from E to W) *Z*-asymmetry throughout the whole study area and are seldom associated with an axial plane cleavage. A mm- to cm-spaced discrete S2 crenulation cleavage develops almost exclusively in the Cretaceous marly limestones of the Upega Formation. Within massive lithologies, such as the Rio di Nava Limestones, D2 structures consist of 'en-échelon' vein

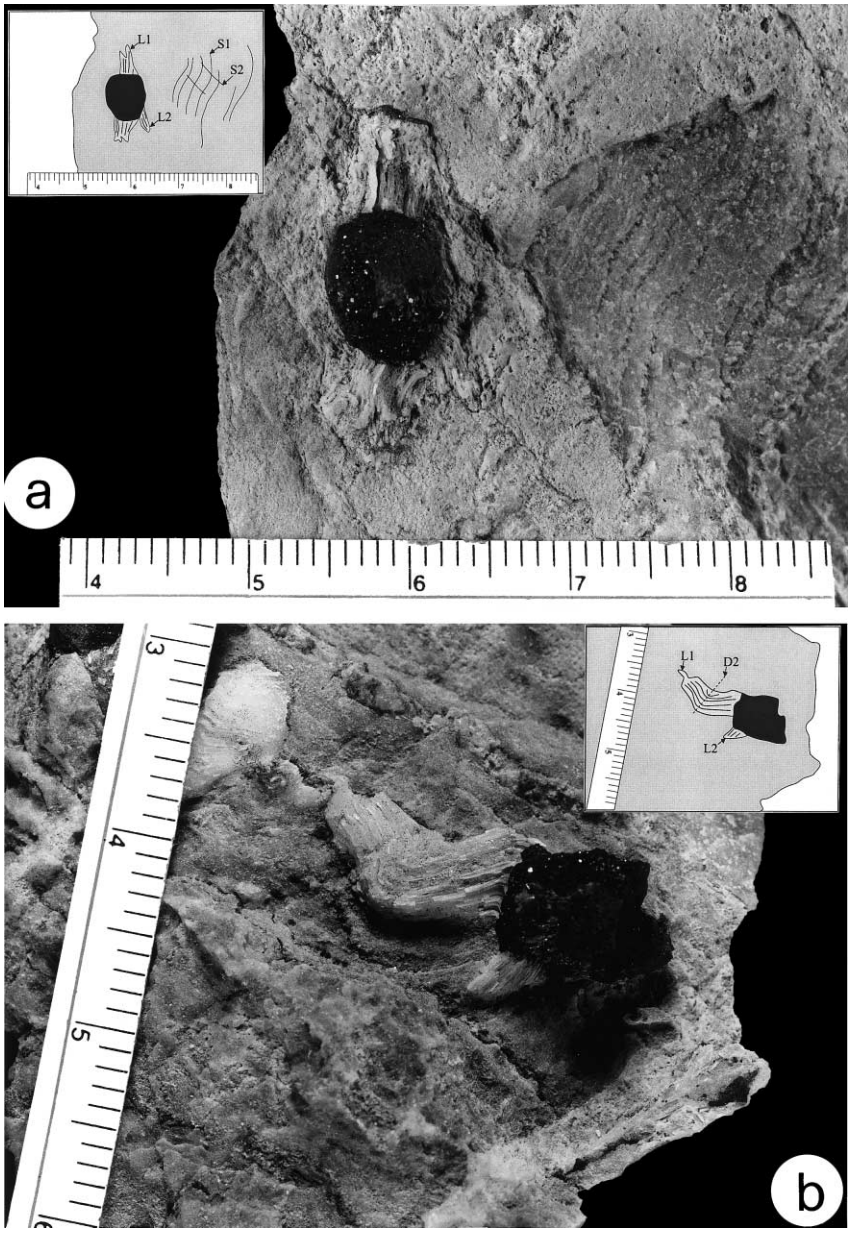

Fig. 6. Composite calcite–quartz fibres in strain fringes around pyrite framboids. (a) Two generations of coaxial fibres, L1 and L2, grew independently, on different sides of the pyrite, parallel to S1 and S2, respectively. (b) L1 fibres deformed during D2 deformation phase (see also Fig. 7). L2 grew parallel to the axial plane of the D2 fold. The scale numbers are centimetres.

systems, whose envelopes are parallel to D2 fold axial planes. The sigmoidal shape of the veins indicates top-to-NE shear sense. Fig. 3c shows the D2 fabric elements and the traces of D2 planar fabric elements. It can be easily observed that the extension of the areas in which continuous S2 has been observed is markedly subordinate to the area in which S1 has been observed.

D3 and D4 structures affect only limited areas and are responsible for small rotations of pre-existing structures. No overprinting relationship has been observed between the two fold systems; consequently the labels ‘D3’ and ‘D4’ here have no chronological meaning. On the mesoscopic scale, D3 and D4 deformations are accommodated by chevron folds or, more frequently, by kink folds which are concentrated close to the hinges of two kilometric-scale open folds (Fig. 3a and c). D3 folds have axial planes dipping 40–60° towards the south (Fig. 5) and have, looking from E to W, an *S*-asymmetry. D4 folds are *Z*-asymmetric looking from N to S and their axial planes dip 70–80° to the east (Fig. 5).

The latest deformational events consist of normal faults with displacements up to tens of meters and variously oriented fracture systems, which strongly affect pre-existing structures.

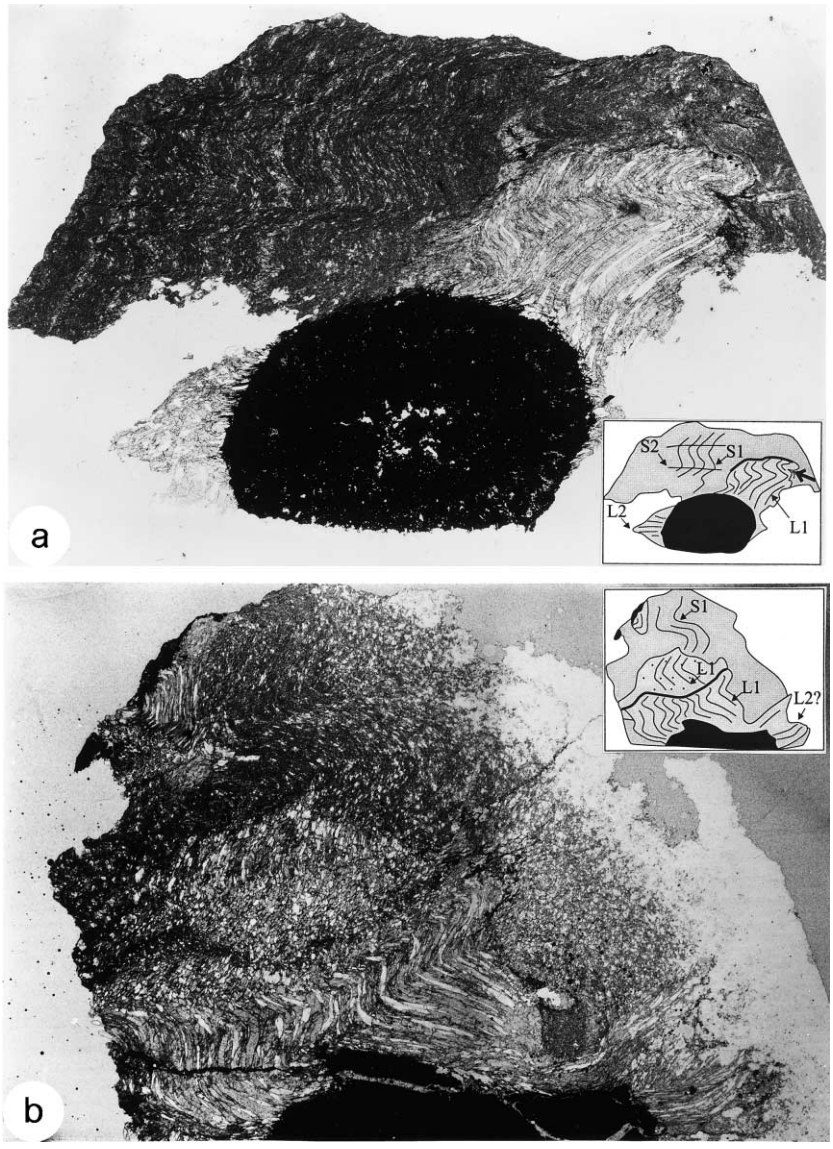

Fig. 7. Microphotographs of curved composite calcite–quartz fibres grown in strain fringes around pyrite framboids embedded in folded matrix rock. (a) Matrix rock shows an S1 cleavage folded during D2 and development of incipient S2 cleavage by mineral rotation and pressure solution along fold flanks. Fibres approximately parallel to S1 and interpreted as L1 lineations are folded with the same style of the matrix. In the inset, a thick line indicates a discontinuity between L1 fibres and S1 cleavage marked by opaque minerals indicating pressure solution. The discontinuity plane occurs on the flank of a D2 fold affecting the fibres compatibly with the common observation that dissolution occurs preferentially in fold limbs (e.g. Passchier and Trouw, 1996, p. 71). This observation reinforces the D2 folding origin of the curvature of L1 fibres. The thick arrows indicates a cuspate–lobate fold at the contact between less competent matrix rock and more competent fibres. Straight fibres growing parallel to S2 cleavage are interpreted as L2 lineations. Plane polarized light. (b) The microphotograph shows a transition from quartz–calcite fibres to matrix rock. The area stippled in the inlet shows characters intermediate between fibres and matrix rock, with composition similar to the fibres and grain similar to the matrix. Lateral continuity can be observed in the D2 folds affecting the S1 cleavage and the L1 fibres, clearly indicating that the L1 fibre curvature is related to D2 folding. The thick line indicates a surface marked by opaque minerals indicating pressure solution. Plane polarized light.

2.2. Lineation analysis

In deformed rocks, different objects can define stretching lineations. In terms of progressive deformation, the objects that form lineations can be defined, with respect to a given deformation increment, as old grains if pre-existing the deformation increment (e.g. minerals, pebbles, fossils) or as new grains if developing during the deformation increment (syntectonic crystals; Ildefonse and Caron, 1987).

Two generations of stretching lineations were recognised in the Monte Marguareis area. The first set (L1) of lineations lies within S1 and, therefore, has been correlated with D1 deformation. L1 stretching lineations commonly plunge towards the NE and SW (Fig. 5). These orientations are obviously the effect of later rotations due to D2–D4 deformations. Two kinds of L1 lineations have been observed.

Stretching lineations due to pressure solution and passive rotation of old grains are exclusively observed in lithologies

characterised by the occurrence of a well developed S1 cleavage. This kind of L1 is easily obliterated in lithologies with a pervasive S2 cleavage (the Cretaceous marly limestones of the Upega Formation). The reorientation, due to folding, of lineations composed of old grains characterised by similar competence, comparable with that of the matrix, is a function of the folding mechanism (Weiss, 1959; Ramsay, 1967). L1 lineations from single D2 folds display small circle patterns on stereographic projections suggesting a flexural slip mechanism for D2 folding.

A second kind of L1 lineation is represented by composite calcite–quartz fibres in veins and strain fringes. These fibres commonly survived D2 deformation and therefore a strain analysis in terms of progressive deformation has been performed for lithologies with abundant strain fringes (Rio di Nava Limestones and Upega Formation limestones), as will be summarised in the next section. During D2 deformation, L1 fibres behaved as old grains with a low competence contrast with respect to the enclosing matrix. Some competence contrast between fibres and matrix existed, however, as indicated by microstructures discussed in the following section. L1 lineations rotated with the S1 cleavage planes and consequently they plunge either towards the SW or NE depending on the D2 fold limb they lie on.

L2 stretching lineations lie on S2 planes and are consequently correlated with D2 deformations. L2 lineations consistently plunge gently (maximum 20°) to the SSW and have been observed only within Cretaceous marly limestones of the Upega Formation, the only lithology characterised by the occurrence of diffuse S2. L2 lineations due to solution and passive rotation of old grains are rare. More frequently, new grain L2 lineations (fibres in strain fringes on pyrite framboids) occur. L2 fibres in pyrite strain fringes have been used for the incremental strain analysis, as described in the next section.

Both L1 and L2 lineations behaved during D3 and D4 deformation as old grains with no competence contrast with respect to the matrix, as suggested by comparable rotations of matrix (cleavages) and lineations.

L1 fibres consist predominantly of calcite, with maximum percentages of quartz around 30%. Older L1 fibres are, generally, almost exclusively composed of calcite (quartz percentage being less than 10–15%). An enrichment in quartz (up to 30%) seems to be observed in more recent fibres (i.e. closer to the pyrite). This slight compositional change of the fibres could be related to compositional (pH) variations of the fluid phases during D1 deformation or alternatively to temperature changes (e.g. Dietrich, 1989). L2 fibre composition does not notably differ from that of late L1 fibres, suggesting that no significant variation of temperature and/or fluid composition occurred between late D1 and D2 phases.

3. Incremental strain analysis

Syntectonic grains (new grains) are frequently associated with rheological grain-scale discontinuities (matrix-inclusion or matrix–matrix interfaces), where decoupling often occurs, allowing the deposition of new grains under the form of strain fringes or vein fibres. Syntectonic fibres have been widely used to determine strain estimates and deformation paths (Durney and Ramsay, 1973; Ramsay and Huber, 1983; Winsor, 1983; Dietrich, 1989; Spencer, 1991) following the assumption of parallelism between fibre growth direction and displacement path of their wall-rock boundaries as they moved apart (Spencer, 1991).

Classical models of fibre growth (Ramsay and Huber, 1983, p. 268) suggest that polyphase deformation develops continuous non-coaxial fibres. This observation has been consistently recorded in several areas from the Alps (e.g. Dietrich, 1989). As an exception, L1 and L2 fibres of the Monte Marguareis area grew on different pyrite sites on S1 and S2 planes. As shown in Fig. 6a, almost linear L1 fibres grew parallel to S1. Subsequent L2 fibres grew unrelated to L1 ones, parallel to S2, on a portion of the pyrite not affected by L1 fibre growth. This situation has been quite commonly observed during strain measurements.

Rarely, curved L1 lineations have been encountered (Fig. 6b). In all of these cases, fibre geometry was related to D2 folding rather than to non-coaxial fibre growth. At the mesoscale, curved L1 fibres show folding style and orientation similar to that of the surrounding S1. The rotational sense of curved L1 fibres observed in the field is consistent with that of D2 folds observed in adjacent rocks. All of the curved fibres observed in the field had curvature consistent with that of D2 phase folds observed in adjacent rocks/outcrops.

In Fig. 6b it can be observed that the axial plane of the fold affecting L1 fibres is parallel to L2, the lineation related to the deformation phase D2.

The deformation-related nature of the L1 fibre curvature has been confirmed by microstructural analyses. Fig. 7 shows microphotographs of curved composite calcite–quartz fibres, embedded in folded matrix rock, grown in strain fringes around pyrite crystals. In both Fig. 7a and b, matrix rock shows an S1 cleavage folded during D2. Fibres approximately parallel to S1 and interpreted as L1 lineations are folded with the same style as the matrix rock. In Fig. 7b, folding can be followed continuously from the fibres to the matrix rock, confirming that the curvature of L1 and of S1 is to be related to D2 folding. Detachments can occur between L1 fibres and matrix because of the activity of a pressure solution mechanism and to rheological contrasts between the more competent fibres and the less competent matrix rock, as indicated by cuspate–lobate structures (Fig. 7a).

The deformation-related nature of the L1 fibre curvature is also consistent with intracrystalline deformation of fibre crystals. As shown in Fig. 8a curved calcite fibres show undulose extinction commensurate with their curvature. Tapered twins are often observed in the calcite fibres. Calcite twins and undulose extinction are commonly observed in older parts of undeformed pressure shadows

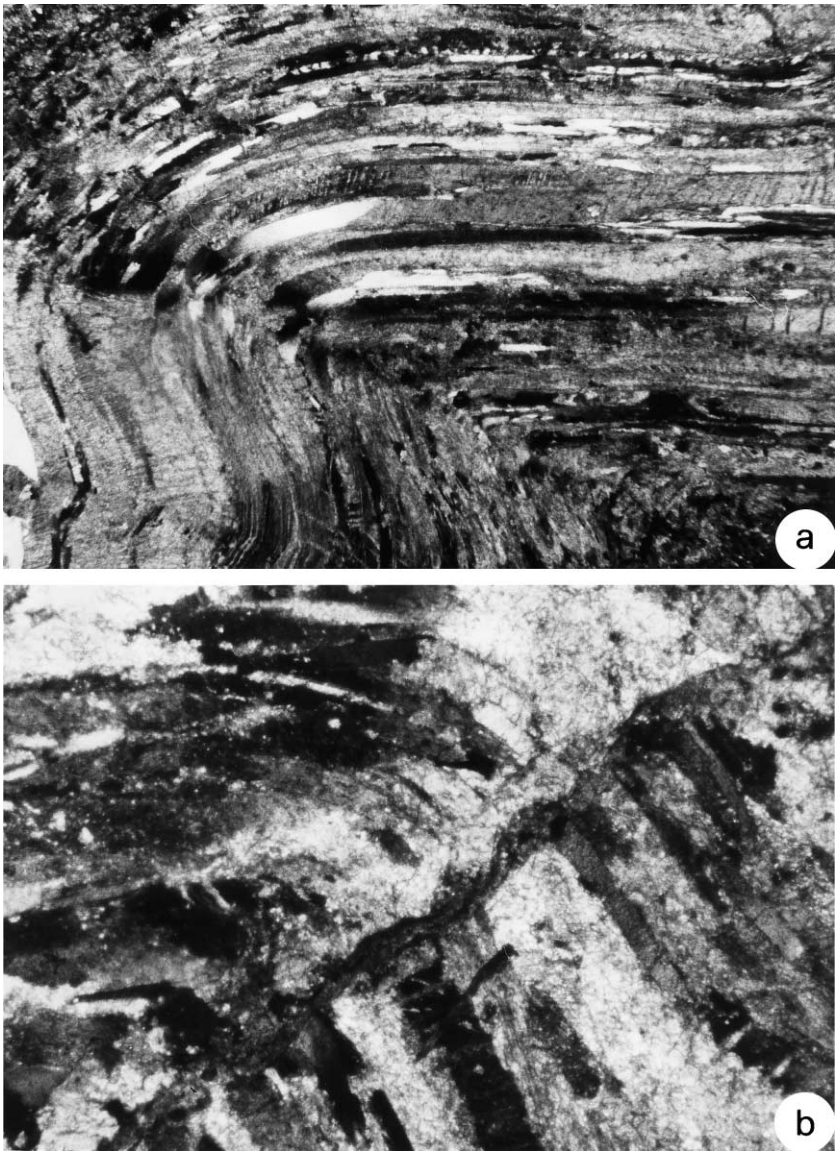

Fig. 8. Microphotographs of curved composite calcite–quartz fibres. The section was obtained from the fibres of Fig. 6b. (a) Calcite fibres show undulose extinction and twins. Quartz fibres do not have undulose extinction and deformation was accommodated by fracturing. Crossed polarised light. (b) Enlargment of the fold hinge of Fig. 8a showing fibre segmentation associated with pressure solution as also indicated by the opaque minerals marking the dissolution surface. Crossed polarised light.

and should not, therefore, be considered diagnostic for folding of fibres (Dietrich, pers. comm.). In the Monte Marguareis case, however, these observations are consistent with the structure shown in Fig. 7 and strongly reinforce the deformation origin of the fibre curvature discussed above (Fig. 7). The frequent observation of undulose extinction and twinning clearly indicates that recovery only slightly affected the fibres after D2 deformation. Locally, however, subgrains and recrystallisation can be observed. Fig. 8a shows that most of the subgrains within calcite crystals are localised at the hinge of the D2 fold affecting the fibres. This is consistent with the migration, during recovery, of dislocations towards areas of maximum curvature (e.g. Passchier and Trouw, 1996, p. 34, fig. 3.14) commonly observed within planar or elongated minerals (e.g. micas and amphiboles). The weak recovery and the occurrence of twinning suggest that conditions during and after D2 deformation were of low temperature (Passchier and Trouw, 1996). Quartz fibres commonly show undulose extinction commensurate to curvature. The curvature of quartz fibres is, however, frequently accommodated by loss of continuity of single fibres, especially at sites of strong curvature. As a consequence, fragments of quartz crystals with the same optical orientation can be only rarely observed on the two limbs of D2 folds affecting the fibres. In these cases, however, a discontinuity can always be observed between the two crystal fragments. The behaviour of quartz fibres during D2 folding confirms that deformation

probably occurred under low temperature conditions. Fibre segmentation is sometimes observed in fold hinges (Fig. 8b). When discussing a possible deformation origin of such discontinuities, it should be borne in mind that fibres are three dimensional structures and that they might, at a certain stage, curve out of the thin section plane. This process would provide an alternative explanation for such discontinuity (see Dietrich, 1989 for a discussion). An alternative explanation to deformation is competitive growth. In this case, individual fibres can be cut out by fibres better oriented for growth. In Fig. 8b, however, the discontinuity is marked by opaque minerals strongly suggesting that pressure solution was active along the discontinuity. This observation is consistent with the D2 fold-related origin of the fibre curvature.

The growth of L1 and L2 fibres in two distinct sites made it easier to perform an incremental strain analysis referring to D1 and D2 deformations. All the fibres considered for strain analysis developed around framboidal pyrites with a size range of about 0.5–1 cm. Framboidal pyrites are considered to have formed early during diagenesis (Love, 1967) and fibres growing on them are assumed to have recorded the whole deformation history. All of the strain analyses were performed on coaxial fibres (similar to those of Fig. 6a) in order to avoid problems with curved fibre interpretation and with the strain analysis method choice. Punctual strain analysis using the Durney and Ramsay (1973) method was carried out at 22 sites located on major structures and distributed uniformly, as far as possible, within the study area. The scarcity of strain measurements at a few sites is due to the difficulty of observing complete fibres.

3.1. Strain analysis results

The results of the strain analysis are summarised in Tables 1 and 2 and are graphically represented in Fig. 3b and c. Tables 1 and 2 contain information about the number of strain analyses carried out at each site, about the arithmetic mean of elongations ($1 + e_1$) measured at single sites and their standard deviations.

It is evident that the small number of data available for single sites do not permit a rigorous statistical treatment. Nevertheless, the use of the average value for the graphical representation of the elongations measured at the different sites is necessary in order to enhance the readability of Fig. 3b and c. Similarly, the standard deviations displayed in Tables 1 and 2 have to be taken as rough estimates of the variability of measurements at single sites.

As already discussed, all of the strain analyses on L1 fibres were performed on the Rio di Nava Limestones and the Upega Formation Limestones. Estimated D1 strain shows a strong strain partitioning between the two lithologies. Cretaceous marly limestones of the Upega Formation account for a mean elongation (calculated with data from the whole study area) of 4.91 (standard deviation of 1.31, equal to 26% of the mean elongation), while the mean elongation for Rio di Nava Limestones is 2.37 (standard deviation 0.29, equal to 12% of the mean elongation). The performed strain analyses suggest, therefore, that the Upega Formation limestones suffered a higher (practically double) amount of stretching than the Rio di Nava Limestones. When the spatial distribution of measured strain is considered (Fig. 3b) it should be noted that the

Table 1
Results of strain analyses performed on L1 fibres. Columns show the number of strain analyses (Data #) carried out in each site (Strain analysis #), the arithmetic mean of elongations ($1 + e_1$) measured at single sites and the standard deviation. UFL: limestones of the Upega Formation; RNL: Rio di Nava Limestones

Strain analysis #	Lithology	Mean elongation (mean $1 + e_1$)	Standard deviation	Data #
1	UFL	7.11	0.95	3
2	RNL	2.77	0.60	3
3	RNL	2.48	0.21	3
4	RNL	1.84	0.12	3
5	UFL	4.48	0.41	3
6	RNL	2.14	–	1
7	RNL	2.72	0.62	6
8	UFL	4.25	0.30	5
9	UFL	4.37	0.62	2
10	UFL	3.96	0.42	5
11	UFL	3.74	0.72	2
12	UFL	3.50	–	1
13	UFL	4.30	0.48	4
14	UFL	4.65	0.63	3
15	UFL	4.22	0.57	3
16	UFL	5.18	0.63	3
18	UFL	4.90	0.23	3
19	RNL	2.37	0.19	4
20	RNL	2.14	0.03	2
21	UFL	5.71	0.90	4
22	UFL	8.45	2.43	5

Table 2
Results of strain analyses performed on L2 fibres. Columns show the number of strain analyses (Data #) carried out in each site (Strain analysis #), the arithmetic mean of elongations ($1 + e_1$) measured at single sites and the standard deviation. UFL: limestones of the Upega Formation

Strain analysis #	Lithology	Mean elongation (mean $1 + e_1$)	Standard deviation	Data #
9	UFL	2.88	0.16	3
10	UFL	2.37	0.18	3
11	UFL	2.61	0.32	5
12	UFL	2.48	–	1
13	UFL	2.40	0.19	4
14	UFL	2.70	0.41	4
15	UFL	2.54	0.21	2
16	UFL	3.25	0.25	2
17	UFL	2.46	0.32	4
21	UFL	3.14	0.60	2
22	UFL	2.80	–	1

highest values of D1 elongations have been measured at sites 1 and 22, close to major (isoclinal) D1 folds, in agreement with intuitive expectations.

Strain analyses also indicate that a strong strain partitioning occurred within the Upega Formation Limestones, while the Rio di Nava Limestones deformed more homogeneously, as can be inferred from the calculated standard deviations. It seems logical that, at outcrops where strain is strongly partitioned, strong variability of measured strain and therefore high standard deviation values are expected. High standard deviations are, in fact, obtained for the Upega Formation Limestones both when the average value of elongation is calculated, as described above, with data from the whole Monte Marguareis area and when standard deviations from single sites are considered. These are summarised in Table 1 and are indicative of strain measurement variability from point to point within single sites. This large strain partitioning can be tentatively related to the higher lithologic heterogeneity which locally characterises the Upega Formation Limestones.

The results of D2 strain analyses are summarised in Table 2 and graphically represented in Fig. 3c. Measurements are available only for the Upega Formation Limestones. From available data it is clear that D2 incremental stretching is usually lower than the D1 one. The mean D2 elongation for the Upega Formation Limestones is 2.69 and the standard deviation is 0.28 (equal to 10% of the mean elongation). D2 stretching is, therefore, approximately half D1 stretching and is characterised by fine homogeneity, as can be observed from the values summarised in Table 2. This finding is consistent with qualitative inferences on strain distribution, which can be done by observing Fig. 3b and c. It appears clearly that the wider extension of the areas where S1 has been observed with respect to those in which S2 is present is related to the higher amount of strain associated with D1 rather than with D2 deformation. This difference is clearly indicated by the strain measurements. From Fig. 3c it also appears clear, as expected, that D2 stretching values are not dependent on the position of the analysis sites with respect to D1 structures. For example, sites 21 and 22, located close to D1 isoclinal fold hinges, display stretching values similar to those of sites far from D1 fold hinges. This clearly confirms the hypothesis, suggested by the meso- and microstructural analyses of lineations, that the fibres observed on S1 and S2 effectively grew during D1 and D2 deformation phases and can be used to reconstruct the strain history associated with these phases.

4. Discussion

In this section, the tectonic implications of the performed strain analyses and the comparison with results of previous works (Menardi-Noguera, 1988; Seno, 1992; Seno et al., 1998) will be discussed. Unfortunately, however, the absence in the Monte Marguareis area of strain markers allowing finite strain analyses prevents a full comparison with previous work.

In order to enhance the readability of the strain analysis results, Fig. 9 shows a fibre map (e.g. Ramsay and Huber, 1983, p. 276, fig. 14.21; Dietrich, 1989). The lines with arrow heads illustrate fibre lengths normalised to a standard pyrite and direction. The orientations of L1 fibres (Figs. 3b and 9) are fairly homogeneous throughout the Monte Marguareis area, the fibres plunging generally NE–SW. Similar lineation orientations were observed in other Brianconnais nappes (Menardi-Noguera, 1988; Seno, 1992). Three dimensional strain analyses performed by the same authors led to the conclusion that, in those areas, the *X*-axis of the finite strain ellipsoid has the same orientation. According to Menardi-Noguera (1988) and Seno (1992), the finite strain ellipsoids obtained were the result of diagenetic compaction and tectonics. Seno et al. (1998) suggest values of 10–25% for pre-tectonic compaction. Both these authors emphasise the parallelism between the *X*-axes and the Eocene regional nappe-emplacement direction (top to SW; Vanossi et al., 1984) suggesting that most of the tectonic component of the strain resulted from deformation in a ductile shear zone possibly induced by the south-westward motion of nappes. This conclusion can be drawn also for the Monte Marguareis Unit when L1 fibres are considered. Both fibre orientations and D1 fold

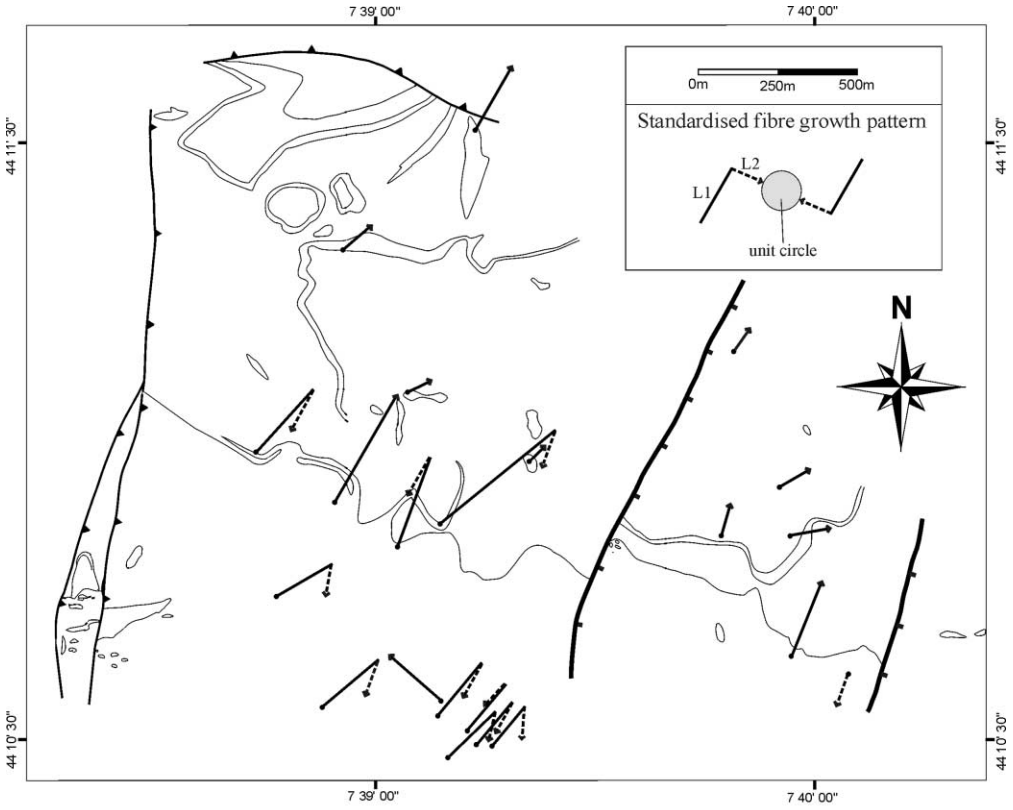

Fig. 9. Fibre map summarising the results of the performed strain analyses. The lines with arrow heads illustrate fibre lengths normalised to the standard pyrite and growth direction (without dip correction). Full lines refer to L1 and dashed lines to L2 lineations.

asymmetry are consistent with this hypothesis, the Helminthoid Flysch constituting the nappe that was thrusted over the Monte Marguareis Unit (Gosso et al., 1983). Merle and Brun (1984), analysing the orientations of stretching lineations within the Parpaillon Nappe of the Helminthoid Flysch, concluded that a 90° rotation of the thrusting direction (from top-to-NW to top-to-SW) occurred through time, as also discussed by Choukroune et al. (1986) for the entire western Alps arc. The top-to-SW thrusting direction of Merle and Brun (1984) is consistent with the direction of L1 in the Monte Marguareis area.

It should be noted that in the areas investigated by Menardi-Noguera (1988) and Seno (1992), the axial planes of D1 folds dip in the direction of nappe motion and D1 fold axes are perpendicular to the *X*-direction. In the Monte Marguareis area, the axial planes of D1 folds generally dip to the W–NW and the fold axes sometimes parallel the elongation direction. Quite a scatter of both fabric elements are observed. Two explanations can be tentatively proposed for this relationship between fabric and strain axes orientation. D1 folds of this area could be parasitic on a major sheath fold. Rare mesoscale sheath folds were observed in extremely ductile layers. A sheath fold geometry of D1 folds has been observed by Seno et al. (1998) in the Mallare unit, belonging to the inner Briançonnais domain. In this unit, D1 deformation developed under high pressure metamorphic conditions. Sheath fold development requires very high strain and progressive rotation of the axes from an initial orientation close to the intermediate axis (*Y*). In the Monte Marguareis case, no large-scale sheath folds were recognised and L1 fibres are, with the exception of tectonically deformed ones, coaxial, suggesting the absence of strong strain tensor rotations. A sheath fold nature of D1 folds cannot, however, be excluded. An alternative explanation could be that D1 folds initiated and developed with axes at low angles with *X*. Grujic and Mancktelow (1995) showed that such geometries can develop within multilayers characterised by high viscosity ratios (ca. 600:1) when initial finite amplitude perturbations are included.

From Fig. 9 it can be observed that the growth directions of L1 and L2 fibres do not differ greatly. The asymmetry of D2 folds is, however, opposite to that of D1 ones. The D2 phase cannot, therefore, be considered as induced by the same tectonic process which determined D1. The L2 lineation orientation (approximately SW–NE) and the D2 folds asymmetry suggest that, during D2, nappe motion was opposite (top-to-NE) to that associated to the D1 phase. This radical kinematic change is symbolised by the sharp bend of the fibre orientations from L1 to L2 displayed in Fig. 9. The D2 thrusting direction is also consistent with the top-to-NE sense of shear indicated by syn D2 'en-échelon' sigmoidal veins observed in the Rio di Nava Limestones. The D2 phase is likely to be the product of a regionally

recognised backthrusting event (e.g. Menardi-Noguera, 1988). As discussed above, the strain associated with D1 is almost twice the magnitude of the D2 one, suggesting a stronger tectonic activity during the former phase. The contribution of D2 to the finite strain ellipsoid cannot be neglected, however, in agreement with the results of Seno et al. (1998) who detected a non-negligible contribution of post D1 deformation to the finite strain ellipsoids that they measured.

5. Conclusions

In the Monte Marguareis cover nappe, two generations of coaxial composite calcite–quartz fibres developed syntectonically during D1 and D2 deformation phases in strain fringes on pyrites. This peculiarity provides a way to quantitatively estimate the incremental strain associated with these deformation phases without the uncertainties related to the classical methods, which are based on the analysis of non-coaxial fibres.

D1 strain estimates were performed on the Rio di Nava Limestones and the Upega Formation Limestones. D1 strain estimates show a strong strain partitioning between the two lithologies, as suggested by the mean elongations obtained for the Cretaceous marly limestones of the Upega Formation and for the Rio di Nava Limestones (4.91 and 2.37, respectively). Within single lithologies, a heterogeneous distribution of D1 strain has been observed throughout the area.

Measurements of D2 incremental elongation are available only for Upega Formation Limestones and indicate that D2 stretching (equal to 2.69) is approximately half that of D1. Measured D2 elongations display higher homogeneity throughout the area. These strain analysis results are consistent with qualitative inferences on strain partitioning between D1 and D2 phases and indicate that the strain measurements performed on the two generations of coaxial fibres drive to valid results.

Both L1 fibre orientation (generally NE–SW) and D1 fold asymmetry suggest D1 deformation occurred in a ductile shear zone, possibly induced by the south-westward motion of nappes, in agreement with previous works (Menardi-Noguera, 1988; Seno, 1992) and consistently with regional tectonics (Vanossi et al., 1984). The L2 lineation orientation (approximately NE–SW) and the D2 fold asymmetry suggest that during D2 nappe, the motion was opposite (top-to-NE) that associated with the D1 phase. As discussed in the previous section, the D2 phase is likely to be the product of a regionally recognised backthrusting event.

Acknowledgements

I would like to kindly thank G. Gosso for introducing me to the geology of the Monte Marguareis area, for fruitful discussions both in the field and in the laboratory and for reading a first draft of the manuscript. G.B. Siletto is thanked for discussions in the field and for reading the manuscript. M.I. Spalla assisted me with discussions on fibre microstructures and with microphotographs. D. Dietrich and R. Lisle are kindly thanked for constructive criticisms that significantly improved the quality of this work. The Gruppo Speleologico Alpi Marittime is thanked for hospitality at the Capanna Scientifica Morgantini. G. Chiodi kindly provided the sample photographs and microphotographs. C. Malinverno skillfully prepared the fibre thin sections. C. Doglioni is kindly thanked for financial support.

References

Brizio, D., Deregibus, C., Eusebio, A., Gallo, M., Gosso, G., Rattalino, E., Rossi, F., Tosetto, S., Oxilia, M., 1983. Guida all'escursione: i rapporti tra la zona Brianzonese Ligure e il Flysch a Elmintoidi, Massiccio del Marguareis (Limone Piemonte–Certosa di Pesio, Cuneo, 14/15 Settembre 1983). Memorie della Società Geologica Italiana 26, 579–595.

Carminati, E., Gosso, G., 2000. Explanatory notes to a new structural map of the Ligurian Briançonnais cover nappe (Conca delle Carsene, Monte Marguareis, Ligurian Alps, Italy). Memorie di Scienze Geologiche 52/1, 93–99.

Choukroune, P., Ballèvre, M., Cobbold, P., Gautier, Y., Merle, O., Vuichard, J.P., 1986. Deformation and motion in the western Alpine arc. Tectonics 5, 215–226.

Dewey, J.F., Helman, M.L., Turco, E., Hutton, D.H.W., Knott, S.D., 1989. Kinematics of the Western Mediterranean. In: Dietrich, D., Park, R.G. (Eds.). Alpine Tectonics. , pp. 421–443 Geological Society Special Publication 45.

Dietrich, D., 1989. Fold-axis parallel extension in an arcuate fold-and-thrust belt: the case of the Helvetic nappes. Tectonophysics 170, 183–212.

Durney, D.W., Ramsay, J.G., 1973. Incremental strains measured by syntectonic crystal growths. In: De Jong, K.A., Scholten, R. (Eds.). Gravity and Tectonics. Wiley, New York, pp. 67–96.

Gosso, G., Brizio, D., Deregibus, C., Eusebio, A., Gallo, M., Rattalino, E., Rossi, F., Tosetto, S., 1983. Due cinematiche possibili per la coppia di falde Brianzonese Ligure–Flysch a Elmintoidi. Memorie della Società Geologica Italiana 26, 463–472.

Grujic, D., Mancktelow, N.S., 1995. Folds with axes parallel to the extension direction: an experimental study. Journal of Structural Geology 17, 279–291.

Guillaume, A., 1969. Contribution à l'étude géologique des Alpes liguro-piemontaises. Documents des Laboratoires de Geologie de la Faculte des Sciences de Lyon 30, 1–658.

Ildefonse, B., Caron, J.M., 1987. The significance of stretching lineations in terms of progressive deformation and finite strain. Geodinamica Acta 1, 161–170.

Laubscher, H., Biella, G.C., Cassinis, R., Gelati, R., Lozej, A., Scarascia, S., Tabacco, I., 1992. The collisional knot in Liguria. Geologische Rundschau 81/2, 275–289.

Love, L.G., 1967. Early diagenetic iron sulphide in recent sediments of the Wash (England). Sedimentology 9, 327–352.

Manivit, H., Prud'Homme, A., 1990. Biostratigraphie du Flysch à Helminthoides des Alpes Maritimes franco-italiennes. Nannofossiles de l'unité de San Remo–Monte Saccarello. Comparaison avec les Flyschs à Helminthoides des Apennins. Bulletin de la Societè Géologique de France VI/1, 95–104.

Menardi-Noguera, A., 1988. Structural evolution of a Briançonnais cover nappe, the Caprauna–Armetta Unit (Ligurian Alps, Italy). Journal of Structural Geology 10, 625–637.

Merle, O., Brun, J.P., 1984. The curved translation path of the Parpaillon nappe (French Alps). Journal of Structural Geology 6, 711–719.

Messiga, B., Oxilia, M., Piccardo, G.B., Vanossi, M., 1981. Fasi metamorfiche e deformazioni alpine nel Brianzonese e nel Pre-Piemontese–Piemontese esterno delle Alpi Liguri: Un possibile modello evolutivo. Rendiconti della Società Italiana di Mineralogia e Petrologia 38, 261–280.

Passchier, C.W., Trouw, R.A.J., 1996. Micro-tectonics. Springer Verlag, Berlin, Heidelberg.

Powell, McA.C., 1979. A morphological classification of rock cleavage. Tectonophysics 58, 21–34.

Ramsay, J.G., 1967. Folding and Fracturing of Rocks. McGraw-Hill, New York.

Ramsay, J.G., Huber, M., 1983. The Techniques of Modern Structural Geology. Volume I: Strain Analysis. Academic Press, London.

Seno, S., 1992. Finite strain and deformation within the Briançonnais Castelvecchio–Cerisola nappe of the Ligurian Alps, Italy. Journal of Structural Geology 14, 825–838.

Seno, S., Dallagiovanna, G., Vanossi, M., 1998. From finite strain data to strain history: a model for a sector of the Ligurian Alps. Journal of Structural Geology 20, 573–585.

Spencer, S., 1991. The use of syntectonic fibres to determine strain estimates and deformation paths: an appraisal. Tectonophysics 194, 12–34.

Vanossi, M., 1972. Rilevamento geologico ed analisi strutturale delle dorsali del Monte Mongioie e del Monte Cimone (Brianzonese Ligure). Atti Istituto di Geologia Università di Pavia 23, 29–71.

Vanossi, M., Cortesogno, L., Galbiati, B., Messiga, B., Piccardo, G., Vannucci, R., 1984. Geologia delle Alpi Liguri: Dati, problemi, ipotesi. Memorie della Società Geologica Italiana 28, 5–75.

Weiss, L.E., 1959. Geometry of superposed folding. Bulletin of the Geological Society of America 70, 91–106.

White, S.H., Wilson, C.J.L., 1978. Microstructure of some quartz pressure fringes. Neues Jahrbuch fuer Mineralogie 134, 33–51.

Winsor, C.N., 1983. Syntectonic vein and fibre growth associated with multiple slaty cleavage development in the Lake Moondarra area, Mount Isa, Australia. Tectonophysics 92, 195–210.